

## CHAPTER 3

# STATE PLANE ANALYSIS, AVERAGING, AND OTHER ANALYTICAL TOOLS

The sinusoidal approximations used in the previous chapter break down when the effects of harmonics are significant. This is a particular problem in the case of discontinuous conduction modes, where harmonics cannot be ignored. To obtain a complete understanding of the behavior of resonant converters, another approach is needed. In this chapter, the fundamental principles necessary for an exact time domain analysis of resonant converters are explained. These principles are used in later chapters to examine not only the series and parallel resonant converters, but also quasi-resonant converters.

The state plane can be used to reduce the complicated tank waveforms of resonant converters to geometry. When properly normalized, the tank waveforms are described by segments of circles, lines, and/or other simple figures in the state plane. Determination of converter steady-state characteristics is often a matter of piecing together these segments, then solving a few triangles or other figures.

Equally important is the use of averaging, in which the dc and low-frequency ac components of the converter terminal waveforms are found while neglecting high frequency switching harmonics. The average output current of the series resonant converter is related to the charge that flows through its output terminals per switching period. This charge also flows through the tank capacitor, where it excites an ac voltage. The load current and tank capacitor voltage magnitude are therefore closely related, and considerable insight can be gained by use of some simple arguments regarding the flow of charge during a switching period. Similarly, the average output voltage of the parallel resonant converter is the volt-seconds (flux linkages) applied to the tank inductor per switching period, and therefore it is also related to the peak tank current. Thus, some simple charge and flux-linkage arguments are discussed in this chapter, and are used in later chapters to easily relate the tank waveforms to the dc terminal voltages and currents.

The various fundamental principles which describe the flow of charge and flux linkages in a resonant circuit, and their relations to the average terminal waveforms, are collected in section 3.1, and are illustrated using the series and parallel resonant converters as examples. Systems of

notation and normalization, a perennial source of confusion in any discussion of resonant converters, are described in section 3.2. In sections 3.3 and 3.4, the ringing responses of series and of parallel resonant tank circuits are derived, and they are plotted in the state plane.

It is apparent that an exact time domain analysis of resonant converters is more complex than the use of the sinusoidal approximations and frequency domain methods of chapter 2. Nonetheless, simple and exact closed-form solutions can be obtained for the many continuous and discontinuous conduction modes of the series resonant converter, as well as for the parallel resonant and many quasi-resonant converters. These ideas are also useful in modeling the dynamics of these converters, and the basic ideas developed in this chapter are used throughout the remainder of this monograph.

### **3.1. Averaging and Related Concepts**

The signals in a power electronics system generally contain substantial switching harmonics. By specification and design, the magnitude of these harmonics must be negligible at the converter output. Hence, when analyzing the behavior of a converter, we usually neglect the switching harmonic components of the converter terminal waveforms, and model only their dominant dc and low-frequency ac components. This simplifies the analysis considerably, and allows a much better understanding of the converter properties.

The basic arguments used to average the converter waveforms were described by Wester and Middlebrook [1]. Although these arguments were originally developed for modeling PWM converters, they also assist the analysis of resonant converters. Averaging the system signals over a period does not significantly alter the waveforms, so long as the period is short compared to the system's natural response times. This is similar to passing the waveforms through a low-pass filter; if the filter corner frequency is sufficiently high, then the important dc and low-frequency ac components are not affected. In particular, it is useful to average the terminal waveforms over one switching period. This effectively removes the switching and ringing harmonics without modifying the desired dc and low frequency ac response, and significantly simplifies the analysis. This approximation is justified because it is normally required that switching harmonics be negligibly small at the load, and therefore sufficient low-pass filtering is incorporated into any well-designed converter.

The implication is that the converter output current can be adequately represented if we simply find the total charge which flows out of the output port during one switching period. Dividing this charge by the switching period yields the average output current. Dual arguments allow representation of the output voltage knowing the total flux-linkages, or volt-seconds, which the converter applies to the output during one switching period. In this section, some basic

principles are discussed which allow the average terminal voltages and currents to be directly related to the tank ringing waveforms.

### ***Averaging: charge arguments***

Let us consider how to average a dependent terminal current  $i_N$  of a switch network, as illustrated in Fig. 3.1. If  $i_N$  is periodic with period  $T$ , then the average value can be written

$$\begin{aligned} \langle i_N \rangle &= \frac{1}{T} \int_0^T i_N(t) dt \\ &= \frac{q_N}{T} \end{aligned} \quad (3-1)$$

where  $q_N = \int_0^T i_N(t) dt$  is the net charge transferred at the port over period  $T$ .

The form  $\langle i_N \rangle = q_N / T$  is useful because, as shown later,  $q_N$  can be related to other salient features of the resonant network waveforms. In particular,  $q_N$  is a function of the change in tank capacitor charge (and hence also the change in tank capacitor voltage) over a portion of the switching period.

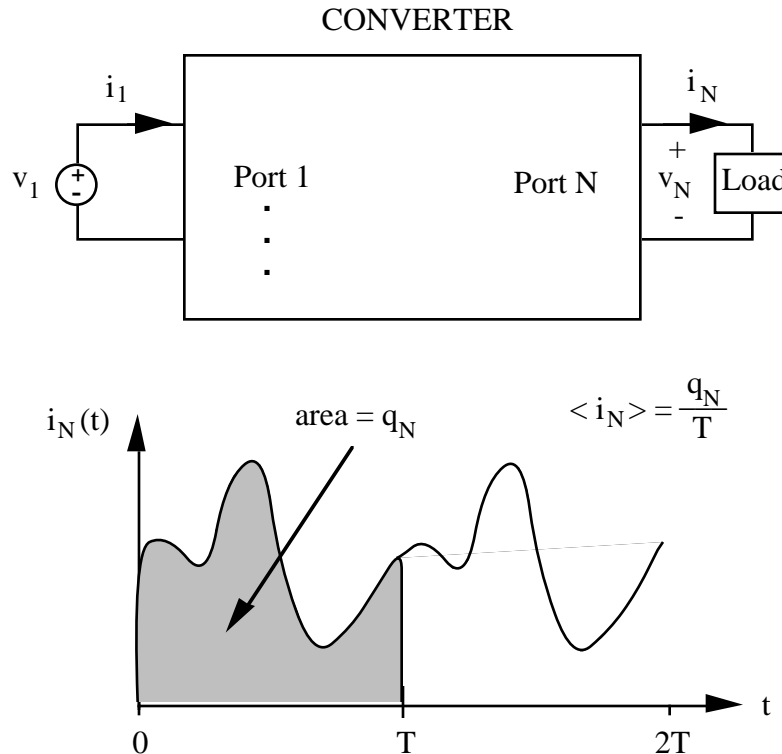


*Fig. 3.1. Arbitrary output of switch network; average output current computed from charge transfer.*

**Averaging: flux-linkage arguments**

Dependent terminal voltages can be averaged using dual arguments. Consider a dependent terminal voltage  $v_N$  of a switch network, as illustrated in Fig. 3.2. If  $v_N$  is periodic with period  $T$ , then the average value can be written

$$\begin{aligned} \langle v_N \rangle &= \frac{1}{T} \int_0^T v_N(t) dt \\ &= \frac{\lambda_N}{T} \end{aligned} \tag{3-2}$$

where  $\lambda_N = \int_0^T v_N(t) dt$  is the net volt-seconds applied at the port over period  $T$ .

The form  $\langle v_N \rangle = \lambda_N / T$  is useful because, as shown later,  $\lambda_N$  can be related to other salient features of the resonant network waveforms. In particular,  $\lambda_N$  is a function of the change in tank inductor flux linkages (and hence also the change in tank inductor current) over a portion of the switching period.

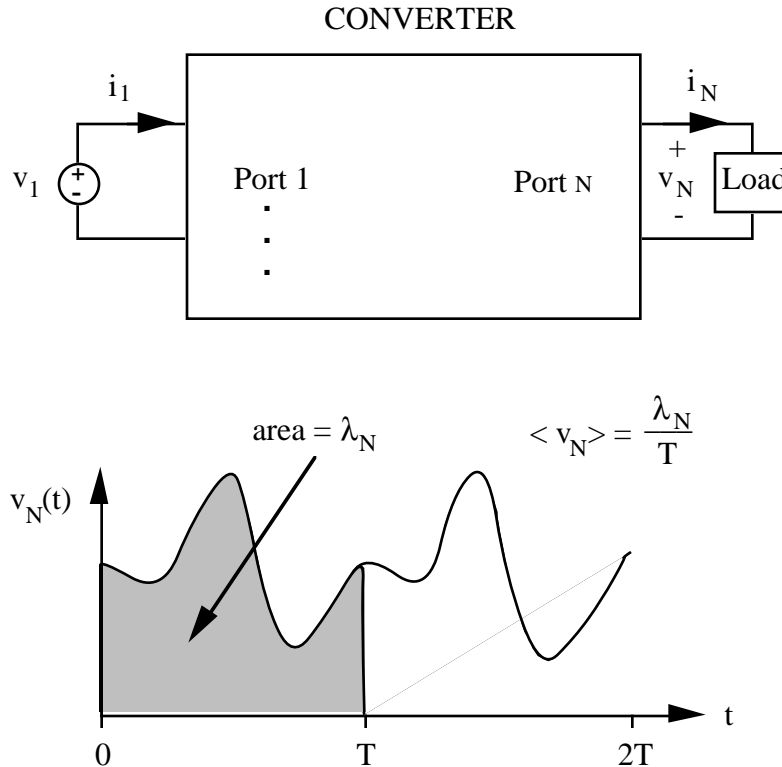


Fig. 3.2. Computation of average terminal voltage  $\langle v_N \rangle$  using flux linkages  $\lambda_N$ .

### Tank capacitor charge variation

Over one switching cycle, charge is transferred from the switch power input, through the tank capacitor, to the output. The amount of charge transfer can be directly related to the capacitor voltage waveform. In particular, over a given interval  $(t_\alpha, t_\beta)$ , if a given amount of charge  $q$  is deposited on the tank capacitor, then we know that the capacitor voltage changes from  $v_C(t_\alpha)$  to  $v_C(t_\beta)$ , where

$$q = C (v_C(t_\beta) - v_C(t_\alpha)) \quad (3-3)$$

Hence, the capacitor voltage initial and final values  $v_C(t_\alpha)$  and  $v_C(t_\beta)$  are related to the charge transfer, and therefore also to the switch average terminal current (by Eq. 3-1).

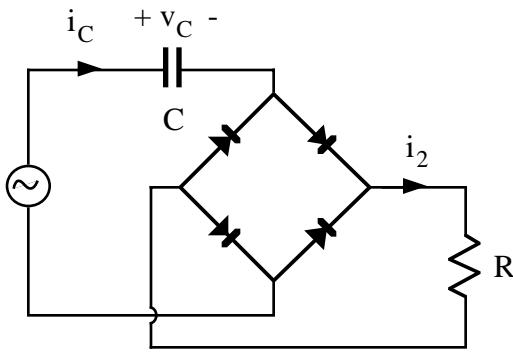


Fig. 3.3. Demonstration of direct relation between dc component of load current and peak-to-peak capacitor voltage.

where

$$q = \int_0^{\frac{1}{2}T} i_2(t) dt$$

During the interval  $0 \leq t \leq T/2$ , the capacitor current  $i_C(t)$  is identical to the bridge rectifier output current  $i_2(t)$ , and hence the same net charge  $+q$  is deposited on the capacitor. The maxima and minima of the capacitor voltage waveform  $v_C(t)$  coincide with the zero crossings of the current  $i_C(t)$ , and hence the capacitor voltage changes from its minimum value  $-V_{CP}$  to its maximum value  $+V_{CP}$  during this interval. The capacitor charge relation is therefore

$$q = C (V_{CP} - (-V_{CP})) = 2CV_{CP} \quad (3-5)$$

Elimination of  $q$  from Eqs. (3-4) and (3-5) yields

$$\langle i_2 \rangle = \frac{4CV_{CP}}{T} \quad (3-6)$$

For example, consider the circuit of Fig. 3.3. It is desired to compute the average, or dc component, of the bridge rectifier output current  $\langle i_2 \rangle$ , and to relate it to the capacitor voltage waveform  $v_C(t)$ . Typical waveforms are sketched in Fig. 3.4. The average value of  $i_2(t)$  is given by:

$$\begin{aligned} \langle i_2 \rangle &= \frac{1}{\frac{1}{2}T} \int_0^{\frac{1}{2}T} i_2(t) dt \\ &= \frac{2q}{T} \end{aligned} \quad (3-4)$$

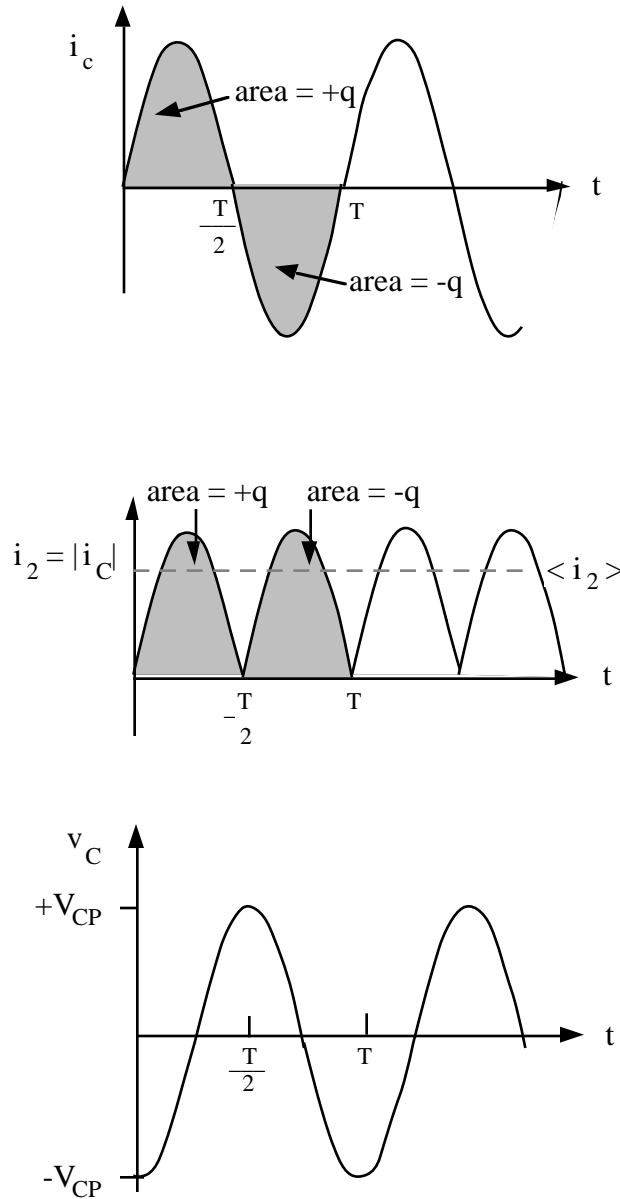


Fig. 3.4. Waveforms for the circuit of Fig. 3.3.

values  $i_L(t_\alpha)$  and  $i_L(t_\beta)$  are related to the volt-second transfer, and hence also to the converter average terminal voltage (by Eq. 3-2).

Hence, the average value, or dc component, of the resistor current  $\langle i_2 \rangle$  and the peak capacitor voltage  $V_{CP}$  are directly related. These arguments are used in chapter 4 to derive a nearly identical relation between the peak tank capacitor voltage and the load current of the series resonant converter.

### Tank inductor flux linkage variation

The dual of the tank capacitor charge relation follows from the definition  $\lambda = L i$ . Inductor flux-linkage  $\lambda$  has the dimensions of volt-seconds, and is the integral of the applied voltage as defined in Eq. (3-2). During one switching cycle, volt-seconds are transferred from the switch power input, through the tank inductor, to the output. So over a given interval  $(t_\alpha, t_\beta)$ , if a given amount of flux linkages  $\lambda$  are stored in the tank inductor, then the inductor current changes from  $i_L(t_\alpha)$  to  $i_L(t_\beta)$ , where

$$\lambda = L (i_L(t_\beta) - i_L(t_\alpha))$$

Hence, the inductor current boundary

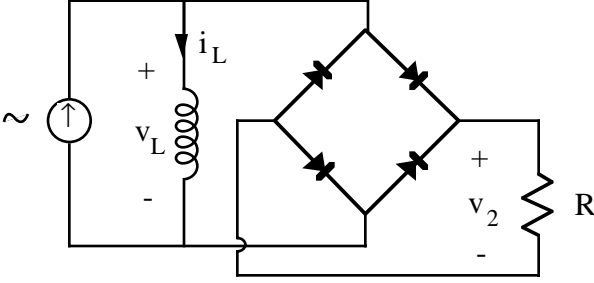


Fig. 3.5. Sinusoidal current source driving an inductor in parallel with bridge rectifier and resistor.

For example, consider the circuit of Fig. 3.5. We wish to compute the average, or dc component, of the bridge rectifier output voltage  $\langle v_2 \rangle$ , and to relate it to the inductor current waveform  $i_L(t)$ . Typical waveforms are sketched in Fig. 3.6. The average value of  $v_2(t)$  is given by

$$\begin{aligned} \langle v_2 \rangle &= \frac{1}{\frac{1}{2}T} \int_0^{\frac{1}{2}T} v_2(t) dt \\ &= \frac{2\lambda}{T} \end{aligned} \quad (3-8)$$

where

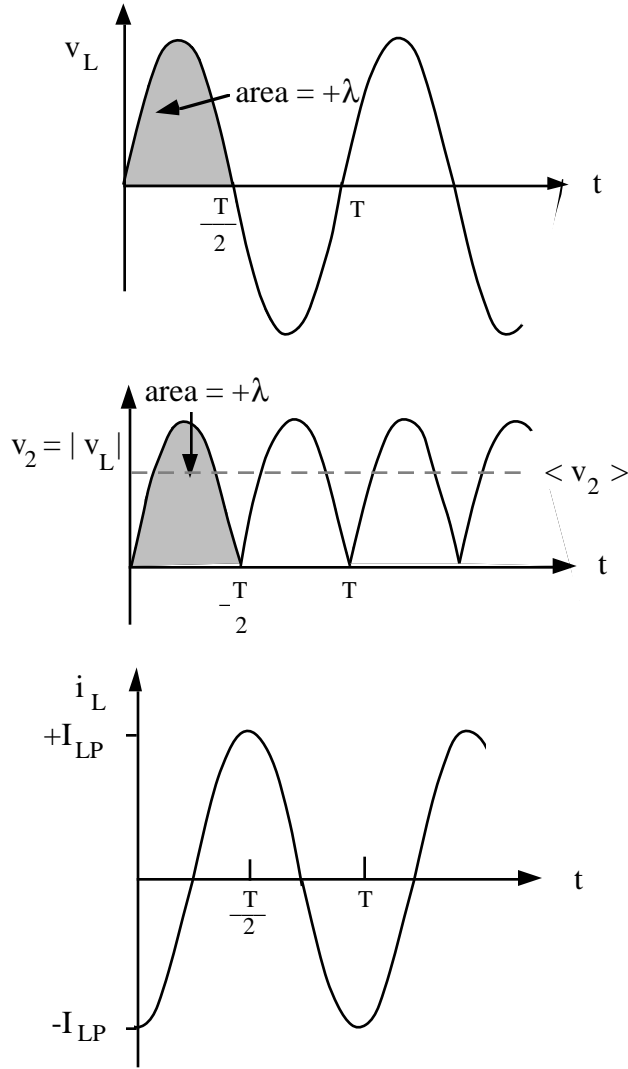
$$\lambda = \int_0^{\frac{1}{2}T} v_2(t) dt$$

During the interval  $0 \leq t \leq T/2$ , the inductor voltage  $v_L(t)$  is identical to the bridge rectifier output voltage  $v_2(t)$ , and hence the same net flux linkages  $+\lambda$  are stored in the inductor. The maxima and minima of the inductor current waveform  $i_L(t)$  coincide with the zero crossings of the voltage  $v_L(t)$ , and hence the inductor current changes from its minimum value  $-I_{LP}$  to its maximum value  $+I_{LP}$  during this interval. The inductor flux linkage relation is therefore

$$\lambda = L (I_{LP} - (-I_{LP})) = 2LI_{LP} \quad (3-9)$$

Elimination of  $\lambda$  from Eqs. (3-8) and (3-9) yields

$$\langle v_2 \rangle = \frac{4LI_{LP}}{T} \quad (3-10)$$



Hence, the average value, or dc component, of the resistor voltage  $\langle v_2 \rangle$  and the peak inductor current  $I_{LP}$  are directly related. Similar arguments are used in chapter 5 to derive a relation between the peak tank inductor current and the load voltage of the parallel resonant converter.

### Kirchoff's laws in integral form

We know from Kirchoff's Current Law (KCL) that the total currents flowing into a given node must be zero:

$$\sum_k i_k = 0 \quad (3-11)$$

The net charge which enters the node over a given interval  $(t_\alpha, t_\beta)$  must also be zero:

$$\sum_k q_k = 0 \quad (3-12)$$

where  $q_k = \int_{t_\alpha}^{t_\beta} i_k(t) dt$

The integral form of Kirchoff's

Current Law is useful for relating terminal charge quantities to the change in tank capacitor charge. For example, consider the circuit of Fig. 3.7. This circuit is similar to the tank circuits of both the parallel resonant converter and the zero-current resonant switch, during one ringing subinterval. In conjunction with the determination of the average input current of this network, we wish to compute the charge contained in  $i_1$  during the given ringing subinterval:

$$q_{1\beta} = \int_{t_\alpha}^{t_\alpha+t_\beta} i_1(t) dt \quad (3-13)$$

By KCL, we know that  $i_1 = i_C + i_2$ . Hence,

$$q_{1\beta} = q_{C\beta} + q_{2\beta} \quad (3-14)$$

where  $q_{C\beta} = \int_{t_\alpha}^{t_\alpha+t_\beta} i_C(t) dt$



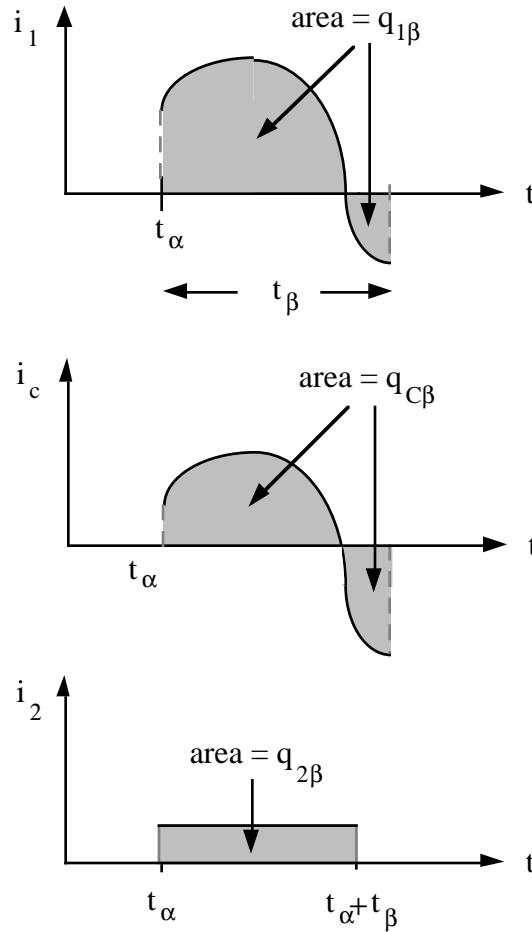
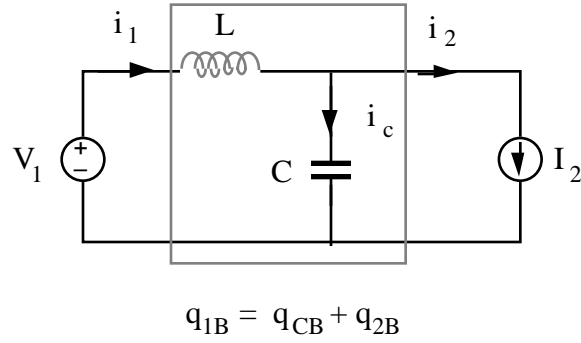


Fig. 3.7. Illustration of use of integral form of KCL for a typical tank network.

and 
$$q_{2\beta} = \int_{t_\alpha}^{t_\alpha+t_\beta} i_2(t) dt$$

Therefore, the ringing interval input charge  $q_{1\beta}$  is related to  $q_{CB}$ , the change in tank capacitor charge over the ringing interval, and to  $q_{2\beta}$ , the charge transferred to the output during the ringing interval. Some of the input charge is stored on the tank capacitor, while the remainder flows to the output.

An integral form of Kirchoff's Voltage Law (KVL) is also useful. The total voltage around a network loop is zero:

$$\sum_k v_k = 0 \quad (3-15)$$

The total volt-seconds applied over a given interval  $(t_\alpha, t_\beta)$  across the elements of this loop must also be zero:

$$\sum_k \lambda_k = 0 \quad (3-16)$$

where  $\lambda_k = \int_{t_a}^{t_b} v_k(t) dt$

When element  $k$  is an inductor or transformer,  $\lambda_k$  has the physical interpretation of winding flux linkages.

The integral form of KVL relates terminal volt-second quantities to the change in tank inductor flux linkages. For example, in conjunction with the determination of the average output voltages of the parallel resonant converter and the zero current resonant switch, we wish to compute the volt-seconds contained in  $v_2$  during the ringing interval (see Fig. 3.8):

$$\lambda_{2\beta} = \int_{t_\alpha}^{t_\alpha+t_\beta} v_2(t) dt \quad (3-17)$$

By KVL, we know that  $v_2 = v_1 - v_L$ . Therefore,

$$\lambda_{2\beta} = \lambda_{1\beta} - \lambda_{L\beta} \quad (3-18)$$

where  $\lambda_{1\beta} = \int_{t_\alpha}^{t_\alpha+t_\beta} v_1(t) dt$

$$\lambda_{L\beta} = \int_{t_\alpha}^{t_\alpha+t_\beta} v_L(t) dt$$

Therefore, the ringing interval output volt-seconds  $\lambda_{2\beta}$  is related to  $\lambda_{L\beta}$ , the change in tank inductor flux linkages over the ringing interval, and to  $\lambda_{1\beta}$ , the volt-seconds applied to the input during the ringing interval. Some of the input volt-seconds are stored in the tank inductor, while the remainder are applied to the switch output.

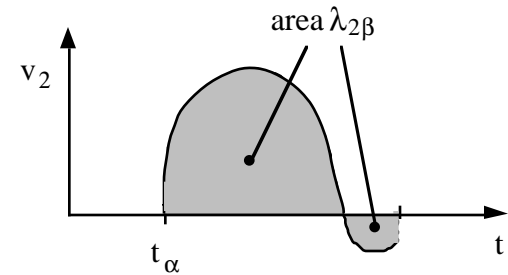
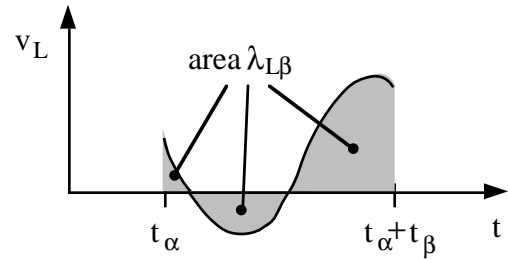
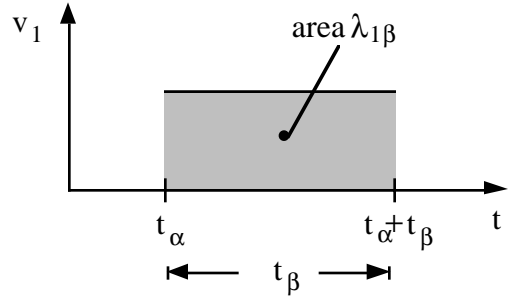
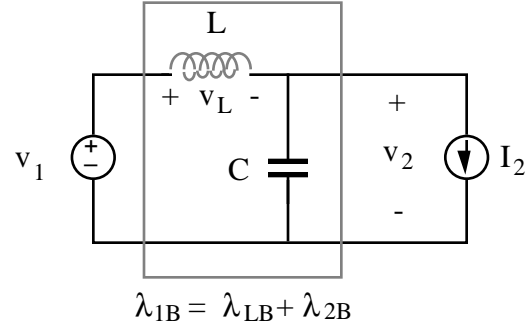


Fig. 3.8. Illustration of the use of the integral form of KVL.

### Steady-state capacitor charge balance

When a capacitor operates with periodic steady-state waveforms, then the initial and final values of the capacitor voltage waveform are identical. In consequence, no net charge is deposited in the capacitor, and the integral of the capacitor current waveform over one complete cycle is zero. The dc component of capacitor current is zero. Formally, this follows from the definition

$$i_C(t) = C \frac{dv_C(t)}{dt} \quad (3-19)$$

Integration over one complete period  $T$  yields

$$v_C(T) - v_C(0) = \frac{1}{C} \int_0^T i_C(t) dt \quad (3-20)$$

In periodic steady state,  $v_C(T) = v_C(0)$ . Hence,

$$0 = \int_0^T i_C(t) dt \quad (3-21)$$

Division by the period  $T$  then shows that the average value,  $\langle i_C \rangle$ , or dc component, must also be zero:

$$\frac{1}{T} \int_0^T i_C(t) dt = \langle i_C \rangle = 0 \quad (3-22)$$

This is the well-known principle of steady-state capacitor amp-second, or charge, balance. It is true for any capacitor which operates with periodic steady-state waveforms.

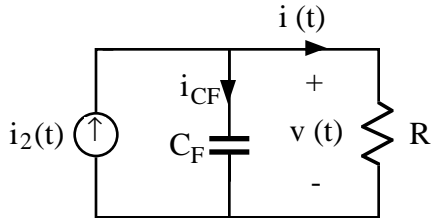


Fig. 3.9 Capacitive filter circuit.

For example, consider the capacitive output filter circuit of Fig. 3.9. In steady state, no net charge is deposited on capacitor  $C_F$  during a switching period, and hence the average rectifier output current  $i_2$  is equal to the dc component  $I$  of the load current  $i(t)$ . By Ohm's law, the dc component  $V$  of the load voltage  $v(t)$  is  $V = IR$ . Hence,

we have

$$V = \langle i_2 \rangle R \quad (3-23)$$

For this example, the input current,  $i_2(t)$ , is a rectified sinusoid

$$i_2(t) = I_{2P} |\sin(\omega_S t)| \quad (3-24)$$

whose average is

$$\langle i_2 \rangle = \frac{1}{T_S} \int_0^{T_S} i_2(t) dt = \frac{2}{\pi} I_{2P} \quad (3-25)$$

Substitution of this expression into Eq. (3-23) yields

$$V = \frac{2}{\pi} I_{2P} R \quad (3-26)$$

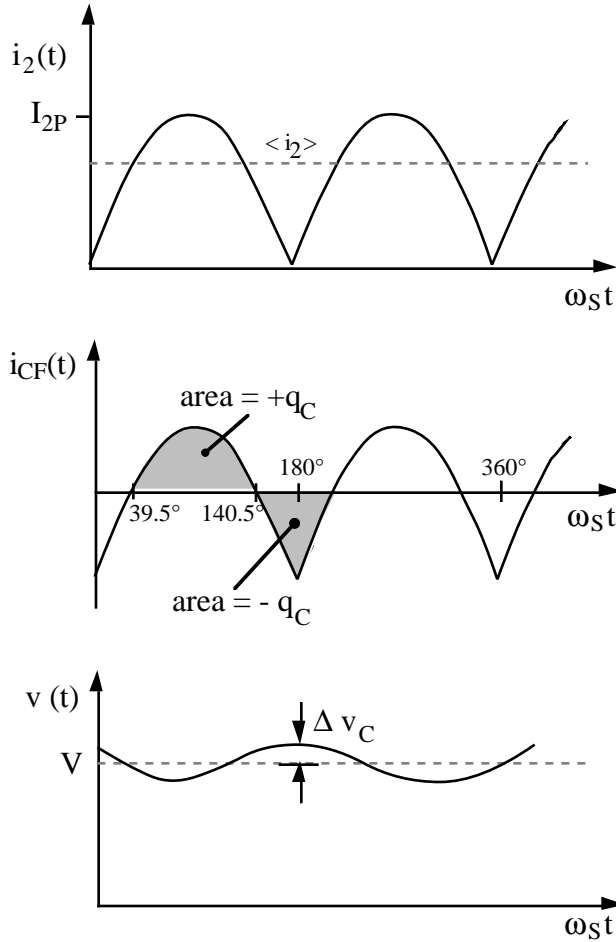


Fig. 3.10. Typical waveforms for the circuit of Fig. 3.9.

Output voltage ripple can also be estimated using charge arguments. In Fig. 3.10, the capacitor current waveform is sketched for the case in which  $C_F$  is large enough that its voltage ripple (induced by the switching harmonics in  $i_2(t)$ ) is small compared to the dc component  $V$ . In this case, the voltage harmonics applied to resistor  $R$  are also small, and hence by Ohm's law the current through  $R$  is essentially dc. Therefore, the dc component of  $i_2(t)$  flows exclusively through  $R$ , while the switching harmonic of  $i_2(t)$  flows overwhelmingly through  $C_F$ . The capacitor current waveform is then given by

$$i_{CF}(t) = i_2(t) - i(t) \cong I_{2P} |\sin(\omega_s t)| - \frac{2}{\pi} I_{2P} \quad (3-27)$$

The capacitor current is positive over the interval  $39.54^\circ < \omega_s t < 140.46^\circ$ . During this interval, the capacitor voltage increases by an amount  $2\Delta v_C$ , from its minimum value to its maximum value. This corresponds to an increase in charge  $q_C$  given by the integral of

Eq. (3-27) over this interval:

$$q_C = \int_{39.54^\circ}^{140.46^\circ} I_{2P} \left( |\sin(\omega_s t)| - \frac{2}{\pi} \right) \frac{d(\omega_s t)}{\omega_s} \quad (3-28)$$

Evaluation of the integral yields

$$q_C = 0.067 I_{2P} T_S \quad (3-29)$$

The peak-to-average capacitor voltage ripple is therefore

$$\Delta v_C = 0.067 \frac{I_{2P} T_S}{2C} \quad (3-30)$$

Or, in terms of the load current,

$$\Delta v_C = 0.0526 \frac{I T_S}{C} \quad (3-31)$$

This gives a simple estimate which is useful for choosing the output filter capacitance. However, it does not include the effects of capacitor esr (equivalent series resistance), which can cause the voltage ripple to be significantly larger than that predicted by Eq. (3-31).

### Steady-state inductor flux-linkage balance

When an inductor operates with periodic steady-state waveforms, then the initial and final values of the inductor current waveform are identical. In consequence, no net flux linkage is induced in the inductor, and the integral of the inductor voltage waveform over one complete cycle is zero. The dc component of inductor voltage is zero. Formally, this follows from the definition

$$v_L(t) = L \frac{di_L(t)}{dt} \quad (3-32)$$

Integration over one complete period  $T$  yields

$$i_L(T) - i_L(0) = \frac{1}{L} \int_0^T v_L(t) dt \quad (3-33)$$

In periodic steady state,  $i_L(T) = i_L(0)$ . Hence,

$$0 = \int_0^T i_C(t) dt \quad (3-34)$$

Division by the period  $T$  then shows that the average value,  $\langle v_L \rangle$ , or dc component, must also be zero:

$$\frac{1}{T} \int_0^T v_L(t) dt = \langle v_L \rangle = 0 \quad (3-35)$$

This is the well-known principle of steady-state inductor volt-second, or flux-linkage, balance. It is true for any inductor which operates with periodic steady-state waveforms.

### 3.2. Normalization and Notation

The geometries of the state plane plots of the next sections are simplified considerably when the waveforms are normalized using a base impedance  $R_{\text{base}}$  equal to the tank characteristic impedance  $R_0$ . The normalizing base voltage  $V_{\text{base}}$  can be chosen arbitrarily, and is usually chosen to be equal to the power input voltage  $V_g$ . Other normalizing base quantities can then be derived:

$$\begin{aligned} \text{base impedance} & R_{\text{base}} = R_0 = \sqrt{L/C} \\ \text{base voltage} & V_{\text{base}} = V_g \\ \text{base current} & I_{\text{base}} = V_{\text{base}} / R_{\text{base}} = V_g / R_0 \\ \text{base power} & P_{\text{base}} = V_{\text{base}} I_{\text{base}} = V_g^2 / R_0 \end{aligned} \quad (3-36)$$

In the system of notation developed at the University of Colorado (CU), the symbol for a normalized voltage contains the same subscripts and case as the original un-normalized voltage, but the character “V” is replaced by “M”. For example,

$$\begin{aligned} M &= V / V_{\text{base}} && \text{normalized load voltage} \\ m_C(t) &= v_C(t) / V_{\text{base}} && \text{normalized tank capacitor voltage} \end{aligned} \quad (3-37)$$

For currents, “I” is replaced by “J”:

$$\begin{aligned} J &= I / I_{\text{base}} && \text{normalized load current} \\ j_L(t) &= i_L(t) / I_{\text{base}} && \text{normalized tank inductor current} \end{aligned} \quad (3-38)$$

When a converter contains a transformer, the base quantities should be referred to the proper side of the transformer by multiplication by the appropriate function of the transformer turns ratio.

Some other authors use the same normalizing base quantities, but denote normalized variables using the subscript “n”. The symbol “q” is also sometimes used to denote the normalized output voltage. Neither of these conventions is used here.

It is convenient to normalize frequency using the tank resonant frequency  $f_0$ , and to convert time to angular form:

$$\begin{aligned} f_{\text{base}} &= f_0 = 1 / 2\pi \sqrt{LC} && \text{base frequency} \\ \omega_0 &= 1 / \sqrt{LC} && \text{tank resonant angular frequency} \\ F &= f_s / f_0 && \text{normalized switching frequency} \\ \alpha &= \omega_0 t_X && \text{angular length of interval } t_X \end{aligned} \quad (3-39)$$

where  $f_s$  is the switching frequency, and  $T_s = 1/f_s$  is the switching period. The following notation is also traditional in the series resonant converter literature:

$$\begin{aligned} \gamma &= \omega_0 T_s / 2 = \pi / F && \text{angular length of one half switching period} \\ \alpha &= \omega_0 t_\alpha && \text{diode conduction angle} \\ \beta &= \omega_0 t_\beta && \text{transistor conduction angle} \end{aligned} \quad (3-40)$$

When performing exact time-domain or state-plane analysis, Q is defined using the actual load resistance R (as opposed to the effective resistance  $R_e$  of chapter 2):

$$\begin{aligned} Q &= R_0 / R && \text{for the series resonant converter} \\ Q &= R / R_0 && \text{for the parallel resonant converter} \end{aligned} \quad (3-41)$$

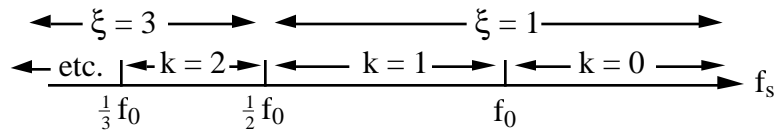


Fig. 3.11. Switching frequency ranges over which various mode indices  $k$  and subharmonic numbers  $\xi$  occur.

Final definitions for the series resonant converter are the mode index  $k$  and subharmonic number  $\xi$ , as follows. The continuous conduction mode  $k$  occurs over the frequency range

$$\frac{f_0}{k+1} < f_s < \frac{f_0}{k} \quad \text{or} \quad \frac{1}{k+1} < F < \frac{1}{k} \quad (3-42)$$

for integer  $k$ . The subharmonic number is then

$$\xi = k + \frac{1 + (-1)^k}{2} \quad (3-43)$$

For example, continuous conduction mode operation at switching frequency  $f_S = 0.4 f_0$  would imply that  $k = 2$  and  $\xi = 3$ .

### 3.3. State Plane Trajectory of a Series Tank Circuit

Let us next examine the time-domain response of a series resonant circuit. A series tank circuit, excited by a constant voltage  $V_T$ , is shown in Fig. 3.12. As shown in the next chapter, the series resonant converter can be reduced to a circuit of this form during each subinterval. The state equations of this circuit are:

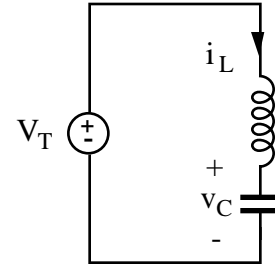


Fig. 3.12. Series tank circuit, excited by constant voltage  $V_T$ .

$$\begin{aligned} L \frac{di_L(t)}{dt} &= V_T - v_C(t) \\ C \frac{dv_C(t)}{dt} &= i_L(t) \end{aligned} \quad (3-44)$$

Let us normalize the state equations according to the conventions of section 3.2. Note that

$$L = \frac{R_0}{\omega_0} \quad \text{and} \quad C = \frac{1}{\omega_0 R_0} \quad (3-45)$$

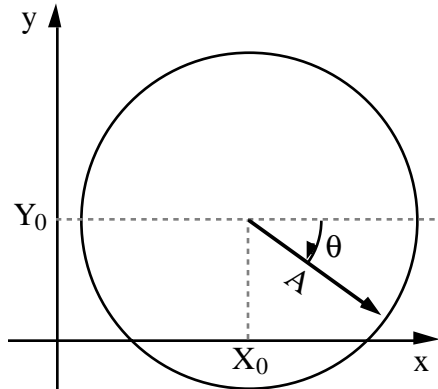
where  $\omega_0$  is the tank angular resonant frequency and  $R_0$  is the tank characteristic impedance, as defined in Eqs. (3-36) and (3-39). Division of Eqs. (3-45) by  $V_g$  and use of the identities (3-46) and (3-36) - (3-39) yields

$$\begin{aligned} \frac{1}{\omega_0} \frac{dj_L(t)}{dt} &= M_T - m_C(t) \\ \frac{1}{\omega_0} \frac{dm_C(t)}{dt} &= j_L(t) \end{aligned} \quad (3-46)$$

where  $M_T = V_T / V_g$ . The solution of this second-order system of linear differential equations is

$$\begin{aligned} m_C(t) &= A \cos(\omega_0 t - \varphi) + M_T \\ j_L(t) &= -A \sin(\omega_0 t - \varphi) \end{aligned} \quad (3-47)$$

where the constants  $A$  and  $\varphi$  depend on boundary conditions. It can be seen that the solution contains a dc term  $m_C = M_T$  (or,  $v_C = V_T$ ) which represents the dc solution of the circuit, plus a sinusoidal term which represents the ac ringing response of the resonant tank.



$$x = X_0 + A \cos(\theta)$$

$$y = Y_0 - A \sin(\theta)$$

Fig. 3.13. Parametric representation of a circle.

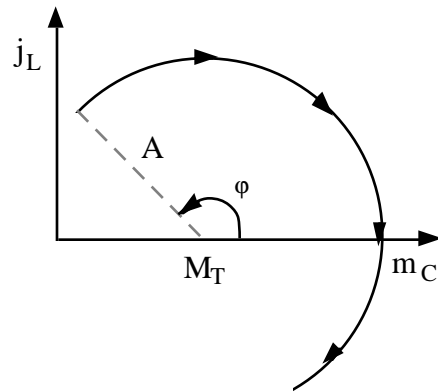


Fig. 3.14. Normalized state plane trajectory for the circuit of Fig. 3.12, corresponding to Eq. (3-47).

### The normalized state plane

The normalized state plane is a plot of  $m_C(t)$  vs.  $j_L(t)$ , with  $t$  as an implicit parameter. As shown in Fig. 3.14, the solution (3-47) above describes a circle in the normalized state plane, of radius  $A$ . If we let the radius go to zero, we can see that the circle is centered at  $m_C = M_T$ ,  $j_L = 0$ , which coincides with the dc solution of the circuit. As time increases, the solution moves in the clockwise direction around the center; this must be true because the capacitor is in series with the inductor, and if the normalized inductor current is positive, then the capacitor charges and  $m_C$  increases. In general, the normalized state plane trajectory of an undamped two-element resonant circuit is circular and is centered at the dc solution of the circuit. The radius depends on the initial values of  $j_L$  and  $m_C$ , and remains constant.

It can also be seen from Eq. (3-47) and Fig. 3.14 that time is related to the angle through which the trajectory moves. During an interval of time  $t_1$ , the trajectory moves through an arc of angle  $\omega_0 t_1$ . So the length of ringing intervals and their angles in the normalized state plane can be easily related. Note, this is not necessarily true for systems other than the resonant tank circuit considered here.

### The tank circuit of the parallel resonant converter

The name of the parallel resonant converter can present some confusion, because although its load is connected in parallel with the tank capacitor, the tank capacitor and inductor are effectively in series. In consequence, the time domain response and normalized state plane trajectory are quite similar to that of the series resonant converter tank circuit.



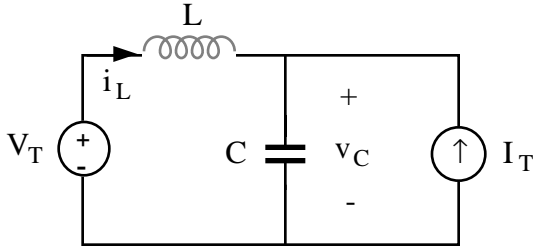


Fig. 3.15. Tank circuit, driven by constant voltage source,  $V_T$ , and constant current source,  $I_T$ .

As shown in chapter 5, during each subinterval of the operation of the parallel resonant converter, its tank circuit can be reduced to a configuration of the form shown in Fig. 3.15. This differs from the circuit of Fig. 3.12 only by the addition of constant current source  $I_T$ . The effect of this extra source is to shift the dc solution of the circuit, and hence also the center of the circular trajectory.

The state equations of the circuit are

$$\begin{aligned} L \frac{di_L(t)}{dt} &= V_T - v_C(t) \\ C \frac{dv_C(t)}{dt} &= i_L(t) - I_T \end{aligned} \quad (3-48)$$

In normalized form, the state equations become

$$\begin{aligned} \frac{1}{\omega_0} \frac{dj_L(t)}{dt} &= M_T - m_C(t) \\ \frac{1}{\omega_0} \frac{dm_C(t)}{dt} &= j_L(t) - J_T \end{aligned} \quad (3-49)$$

where  $J_T = I_T R_0 / V_g$ . The solution is

$$\begin{aligned} m_C(t) &= M_T + (m_C(0) - M_T) \cos(\omega_0 t - \phi) + (j_L(0) - J_T) \sin(\omega_0 t - \phi) \\ j_L(t) &= J_T + (j_L(0) - J_T) \cos(\omega_0 t - \phi) - (m_C(0) - M_T) \sin(\omega_0 t - \phi) \end{aligned} \quad (3-50)$$

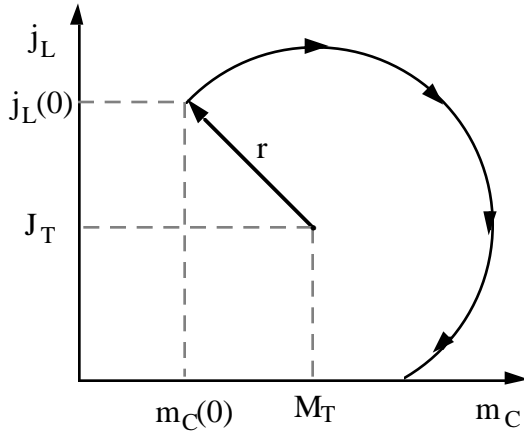


Fig. 3.16 Normalized state plane trajectory for the circuit of Fig. 3.15.

As shown in Fig. 3.16, this represents a circular arc centered at the dc solution  $m_C = M_T$ ,  $j_L = J_T$ , whose radius  $r$  depends on the initial conditions and is given by

$$r = \sqrt{(m_C(0) - M_T)^2 + (j_L(0) - J_T)^2} \quad (3-51)$$

As in the case of the circuit of Fig. 3.12, the length of ringing intervals and their angles in the normalized state plane can be easily related. During an interval of time  $t_1$ , the trajectory moves through an arc of angle  $\omega_0 t_1$ .

All of the fundamental concepts necessary for an exact analysis of the series, parallel, and other resonant converters have now been discussed. Various arguments involving the flow of charge and flux-linkages can be used to relate the tank waveforms to the average terminal voltages and currents of the converter. The waveforms can be normalized, which causes the state plane trajectories to assume circular paths. As seen in the next two chapters, these concepts allow

closed-form analytical solution of the characteristics of the series and parallel resonant converters in a direct manner. They also aid in the understanding of resonant switch converters.

#### REFERENCES

- [1] G.W. Wester and R.D. Middlebrook, "Low Frequency Characterization of Switched Dc-Dc Converters," *IEEE Transactions on Aerospace and Electronic Systems*, vol. AES-9, May 1973, pp. 376-385.
- [2] Steven G. Trabert and Robert W. Erickson, "Steady-State Analysis of the Duty Cycle Controlled Series Resonant Converter", IEEE Power Electronics Specialists Conference, 1987 Record, pp. 545-556.
- [3] R. Oruganti and F.C. Lee, "Resonant Power Processors, Part 1: State Plane Analysis," *IEEE Transactions on Industry Applications*, vol. IA-21, Nov/Dec 1985, pp. 1453-1460.
- [4] R. Oruganti and F.C. Lee, "State Plane Analysis of the Parallel Resonant Converter," IEEE Power Electronics Specialists Conference, 1985 Record, pp. 56-73, June 1985.
- [5] C.Q. Lee and K. Siri, "Analysis and Design of Series Resonant Converter by State Plane Diagram," *IEEE Transactions on Aerospace and Electronic Systems*, vol. AES-22, no. 6, pp. 757-763, November 1986.